Journal of the Acoustical Society of America, Vol. 104, 1998

Ultrasound Induced Cavitation and Sonochemical Yields

Cuiling Gong and Douglas P. Hart

Massachusetts Institute of Technology
Department of Mechanical Engineering
Cambridge, MA 02139-4307

ABSTRACT

The introduction of a strong acoustic field to an aqueous solution results in the generation of cavitation microbubbles. The growth and collapse of these microbubbles focuses and transfers energy from the macro-scale (acoustic wave) to the micro-scale (vapor inside the bubbles) producing extremely high localized pressures and temperatures. This unique energy focussing process generates highly reactive free radicals that have been observed to significantly enhance chemical processing.

This paper presents a model that combines the dynamics of bubble collapse with the chemical kinetics of a single cavitation event. The effects on sonochemical yields and bubble dynamics of gas composition and heat transfer are assessed and compared with previous theoretical and experimental studies. Results from this model are used to explain unusual experimentally observed sonochemical phenomena.

PACS numbers: 43.25Yw, 43.35E, 82.30cf

Keywords: Cavitation, Ultrasound, Sonochemistry, Bubble dynamics

NOMENCLATURE

h_k	Species specific enthalpy
k	The k-th species
v	Velocity of the bubble wall
K	Thermal conductivity
P_b	Pressure within the bubble
P_∞	Pressure at the infinity
R	Bubble radius
T	Temperature
V	Volume of a bubble ($\frac{4}{3}\pi R^3$)
W	Mean molecular weight of all species
Y_k	Species mass fraction
δr	Thermal boundary layer thickness
μ	Fluid viscosity
ρ	Mean density of all species
ρ_l	Fluid density
$\Re$	Universal gas constant
$\dot{\omega}_k$	Chemical production rate

1 INTRODUCTION

Ultrasound enhances chemical reactions in a solution through the generation of cavitation microbubbles. The growth and collapse of these microbubbles result in the transfer and focusing of energy from the macroscale motion of the acoustic transducer to the microscale vapor inside the bubbles. During collapse, extremely high pressures on the order of hundreds of atmospheres and extremely high temperatures on the order of thousands of degrees Kelvin are generated in the vapor phase inside the bubble. Consequently, highly reactive free radicals are produced. This unique energy focusing mechanism provides a means of reacting compounds in an aqueous solution. The potential applications of this technology range from degradation of environmental pollutants to drug synthesis for medical treatment.

Sonochemistry, the chemistry associated with ultrasound, is governed by parameters that include, amplitude and frequency of an applied sound field, temperature, surface tension, vapor pressure, gas content and nuclei density of the solution as well as vessel and probe geometry[1]. The close coupling of these parameters as well as the small size and high oscillation frequency of the microbubbles, and the low species concentration inside any single bubble makes experimental and theoretical investigations of sonochemistry extremely difficult. Nonetheless, there have been a number of investigations from various perspectives each providing useful insight into this fascinating phenomenon.

The dynamics of cavitation bubbles in the absence of chemical reactions has been extensively investigated largely because of its importance to ship propulsion and hydraulic pumping. Rayleigh and later Plesset studied the dynamic behavior of a single cavitation bubble leading to the well-known Rayleigh-Plesset equation[2,3]. Gaitan *et al.*, Matsumoto, and Takemura studied the effects of thermal conduction, vapor condensation and diffusion of non-condensable gas on bubble motion. They concluded that thermal conductivity and initial bubble radius are critical parameters in predicting bubble collapse pressures and temperatures[4,5].

Theoretical models of bubble dynamics have become increasingly comprehensive and accurate providing useful insights into sonochemical phenomena. At the same time, experimentalists have extensively investigated the production of free radicals in ultrasonic fields. Anbar and Pecht investigated the location of the sonochemical formation of hydrogen peroxide and found that H_2O_2 is produced in the cavitation bubbles and not in the liquid phase[6]. Hart and Henglein conducted extensive experiments of the production rate of H_2O_2 when water is sonicated under various gas mixtures[7,8]. Suslick *et al.* investigated the application of sonochemistry in numerous commercial processes and found that either better quality of the products were achieved or simpler experimental conditions were required when ultrasound was introduced[9,10,11]. In addition, Suslick along with Flint analyzed the sonoluminescence spectrum from silicone oil and estimated the effective cavitation temperature to be approximately 5000 °K[12].

Several recent studies have attempted to explain the interactions between bubble motion and chemical reactions. Arguably, the most insightful and certainly the most extensive of these studies is the one by Kamath, Prosperetti and Egolfopoulos[13]. Using a comprehensive thermal model, they estimate the production of radicals from the dissociation of water vapor in an oscillating argon bubble. They conclude that the bubble radius and heat transfer between the bubble and the liquid are critical parameters for sonochemical yields. Despite the detail of this model, it does not account for the coupling of bubble dynamics with chemical kinetics. Thus,

the effects of chemical reactions on the temperature field of the bubble are not taken into account. Furthermore, constant gas properties are assumed. Properties, such as enthalpy, entropy, and the specific heat, however, vary significantly with temperature and are important in predicting sonochemical behavior.

This paper presents a model that couples chemical kinetics occurring in a cavitation bubble directly with bubble dynamics. Results from this model are compared with results from the model of Kamath *et al.* and experimental results obtained by Hart and Henglein. Such a model provides a means of investigating the chemical kinetics that takes place at each stage of the bubble collapse process. By combining the extensive chemical kinetics program developed at Sandia National Laboratory, CHEMKIN, to a detailed bubble dynamic model, key parameters such as dissolved gas content, initial bubble radius, acoustic pressure, acoustic frequency, and solution temperature and composition can be systematically investigated. This model provides a means of resolving fundamental scaling relationships and helps explain unusual sonochemical phenomena.

2 MODEL

The model presented herein is derived from the conservation equations of mass, momentum, and energy governing sonochemistry. The dynamic behavior of the bubble wall is described by the Rayleigh-Plesset equation,

$$\frac{\partial \upsilon}{\partial t} = \frac{1}{R}\left(\frac{P_b - P_\infty - 4\mu \upsilon / R}{\rho_l} - \frac{3}{2}\upsilon^2 \right) \tag{1}$$

and the conservation of species is given by

$$\frac{\partial Y_k}{\partial t} = \frac{\dot{\omega}_k \cdot W_k}{\rho} \tag{2}$$

Direct coupling of chemical kinetics and bubble dynamics is made through the energy equation,

$$\rho \frac{dh}{dt} - \frac{dP_b}{dt} = \nabla \left(K \cdot \nabla T \right) \tag{3}$$

Note that $h = \sum Y_k h_k$ and $h_k = C_{pk} T$. Substitution of h and h_k into Equation (3) yields

$$\frac{\partial P_b}{\partial t} = \rho \left(\sum_k h_k \frac{\partial Y_k}{\partial t} + \bar{c}_p \frac{\partial T}{\partial t} \right) - K \frac{\Delta T}{(\delta r)^2} \tag{4}$$

where $\bar{c}_p = \sum Y_k C_{pk}$ and ΔT is the bulk temperature difference between the bubble and the solution. Note that the heat conduction term in Equation (3) has been linearized in Equation (4) based on a thermal boundary layer of thickness δr. This linearization greatly simplifies calculations eliminating the need to accurately model species transport within the bubble. The thermal boundary layer thickness, δr, is based on results from the model of Kamath *et al.* and is typically 20% of the bubble radius.

Differentiating the equation of state, $P_b V = m \Re T / W$, with respect to t gives

$$\frac{\partial T}{\partial t} = -WT\left(\sum_k \frac{1}{W_k}\frac{\partial Y_k}{\partial t}\right) + \frac{4\pi R^2 W}{m\Re}\left(\frac{R}{3}\frac{\partial P_b}{\partial t} + P_b\frac{\partial R}{\partial t}\right) \tag{5}$$

The time derivative of temperature can be obtained by rearranging Equation (4) and Equation (5),

$$\frac{\partial T}{\partial t} = \left(-WT\sum_k \frac{1}{W_k}\frac{\partial Y_k}{\partial t} + \frac{W}{\Re}\sum_k h_k\frac{\partial Y_k}{\partial t} + \frac{3T}{R}\frac{\partial R}{\partial t}\right)\Bigg/\left(1 - \frac{W}{\Re}\bar{c}_p\right) \tag{6}$$

The mass fraction of each species is obtained from chain reaction mechanisms. The chemical reactions that occur in the simplest sonochemical systems are exceedingly complicated with nineteen forward/backward reaction mechanisms occurring in a pure water system alone. All nineteen reaction mechanisms are accounted for in the present model. Of these mechanisms, seven account for most of the chemical kinetics occurring during sonocation. These seven primary reaction mechanisms are,

$$H_2O \Leftrightarrow H^\bullet + OH^\bullet \tag{7}$$

$$H^\bullet + H^\bullet \Leftrightarrow H_2 \tag{8}$$

$$OH^\bullet + OH^\bullet \Leftrightarrow H_2O_2 \tag{9}$$

$$H^\bullet + O_2 \Leftrightarrow HO_2^\bullet \tag{10}$$

$$H^\bullet + HO_2 \Leftrightarrow H_2O_2 \tag{11}$$

$$HO_2^\bullet + HO_2^\bullet \Leftrightarrow H_2O_2 + O_2 \tag{12}$$

$$H_2O^\bullet + OH^\bullet \Leftrightarrow H_2O_2 + H^\bullet \tag{13}$$

The rate coefficients for the reactions are given in the temperature dependent Arrhenius form

$$K_i = A_i T^{\beta_i} e^{\left(-\frac{E_i}{\Re T}\right)} \tag{14}$$

where A_i, β_i, and, E_i are reaction coefficients of the *ith* species.

The dynamics of a collapsing bubble in pure water and the resulting sonochemical yield were predicted by iteratively stepping in time, solving the equations governing bubble motion, and correcting internal temperatures and pressures based on predicted species behavior. CHEMKIN, a program developed at Sandia National Laboratories[14], was incorporated into the present bubble model for the analysis of gas-phase chemical kinetics. CHEMKIN processes reaction mechanisms and provides the appropriate thermodynamic data for the species involved. The bubble dynamic model, in turn, takes the thermodynamic data produced by CHEMKIN and solves for the bubble radius, velocity of the bubble wall, temperature and pressure inside the bubble as well as the production of each chemical species.

Several approximations are made in the current model:

1. Bubbles remain spherically symmetric.

The assumption of spherical bubble collapse is widely used because of its simplicity. It is not valid when a bubble collapses near a solid surface or in the vicinity of other bubbles where severe distortion in bubble shape can occur. The physics of asymmetric bubble collapse is poorly understood and it is not clear that asymmetric bubble collapse can result in sufficient pressures and temperatures to impact sonochemical yields.

2. Surface tension is negligible.

   This approximation is based on a study by Kuvshinov[15] in which surface tension was shown to have a negligible effect on the dynamics of bubble collapse in water.

3. The thermodynamic properties of chemical species are calculated using a polynomial fit of data available in a temperature range between 300 °K and 5000 °K.

   The thermodynamic database provided by Sandia National Laboratory has data in a temperature range between 300 °K and 5000 °K. When the bubble vapor temperature is above 5000 °K, thermodynamic data are estimated using a polynomial relation obtained between 300 °K and 5000 °K. During the final stages of collapse when the internal temperature of the bubble is above 5000 °K, the bubble collapse rate is faster than the chemical reaction rate. Bubble chemistry, in essence, is frozen at this relatively early stage of bubble collapse. Thus, assuming no unforeseen trends in species behavior, the limited database available has little effect on predictions of sonochemical yields.

4. No mass transfer between the bubble and the surrounding fluid.

   As shown by Gaitan et al., Matsumoto, and Takemura, the effects of vapor condensation and diffusion of non-condensable gas have a significant effect on bubble motion[4,5]. Undoubtedly, it will also have a significant effect on bubble chemistry. These effects, however, occur over multiple cycles of oscillation altering the size of the bubble and changing the internal composition of the vapor phase. Little is known about the accuracy of existing mass transfer models. To separate the physics of mass transfer from the fundamental physics of bubble chemistry occurring in a few oscillation cycles, the current model takes, as input, bubble vapor composition and neglects mass transfer during bubble expansion and collapse. Deviations from initial vapor composition are assumed to be slight within a few bubble oscillation cycles.

5. Uniform pressure inside the bubble.

   The assumption of spatial uniform pressure inside the bubble is valid as long as inertia effects are negligible and the velocity of the bubble wall is below the speed of sound in the vapor-gas mixture. This assumption is justified in detail in the paper by Kamath et al.[13].

6. Thermal conduction occurs through a thin thermal boundary layer between the bubble and the solution.

   The assumption that temperature discontinuity is localized within a thin layer is justified by Fujikawa and Akamatzu[16]. Kamath et al.[13], using a more comprehensive model, show that the temperature profile in the vapor phase of the bubble is roughly uniform except for a strong thermal boundary layer at the wall. In addition, they show that the thermal boundary layer thickness near the wall relative to bubble radius is roughly independent of initial conditions. In order to reduce computational intensity, the current model predicts heat transfer through the bubble wall based on a linear approximation of the shape of the temperature profile predicted by Kamath et al.. This approximation allows one-dimensional chemical kinetics

calculations and eliminates the need to account for species convection and diffusion within the bubble.

3 RESULTS

3.1 Bubble Dynamics

The model was used to predict the reactions in an argon bubble in water sonicated at a frequency of 21 *kHz*. An argon bubble was chosen as the focus of this study because of the simple chemical reactions that occur during sonication. In addition, it allows comparison between the current model and that of Kamath *et al.*.

Figure 1(a) shows the normalized radius *(solid line, left scale)* and internal pressure *(dotted line, right scale)* as a function of time calculated using the current model in one cycle of the driving pressure. The bubble has an initial radius of 26 μm and is driven by an acoustic field with a pressure amplitude of 0.93 *atm* and a frequency of 21 *kHz*. Typical features of bubbles oscillating in a sound field are illustrated in this figure. The bubble expands slowly when the pressure inside the bubble is higher than the ambient pressure. It continues expanding even when the inside pressure is lower than the driving pressure due to the inertia of the water until a maximum radius of $2.4R_o$ is reached. The bubble then collapses violently and reaches a minimum radius of $0.4R_o$. The time scale of collapse is roughly one third that of expansion with the finial stage of collapse in which temperatures are sufficient to disassociate water vapor occurring in a few microseconds. The maximum pressure reached, on the order of 100 bar, occurs during the first collapse of the bubble. There are three rebounds following the initial collapse. With each rebound, the collapse becomes weaker as can be seen from the significant decrease in rebound temperature and pressure.

Figure 1(b) shows the results obtained from the Kamath *et al.*'s model under the same conditions. In general the bubble behavior predicted by the two models is very similar especially the bubble radius as a function of time. Differences in the peak temperature and the peak pressure reached during collapse can be attributed to the addition of detailed temperature and pressure dependent gas properties and the coupling of chemical kinetics to bubble dynamics taken into account in the current model. These additions only slightly alter bubble behavior but are critical in predicting sonochemical yields.

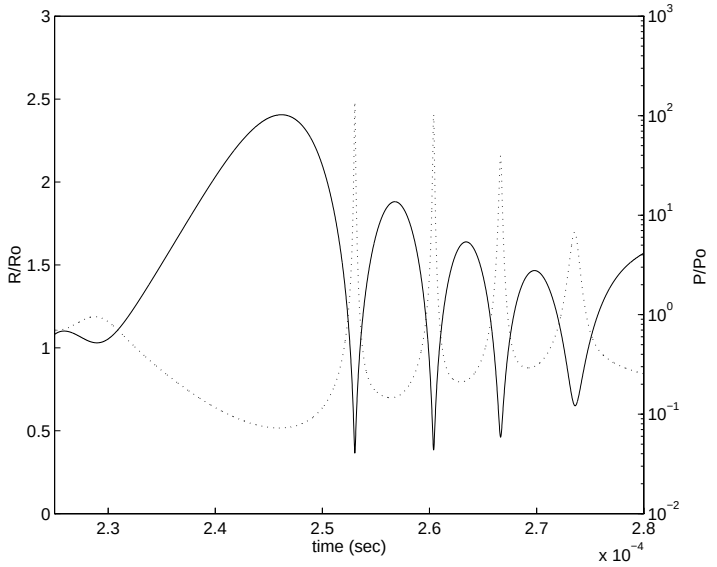

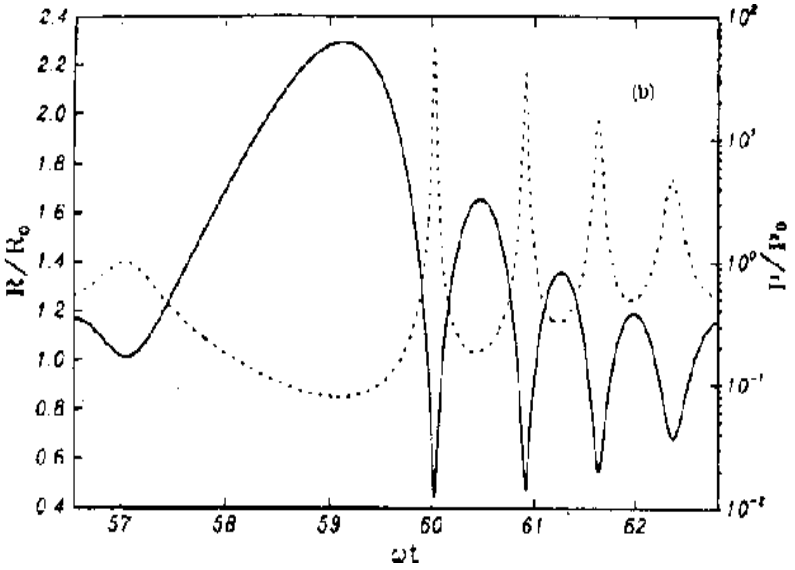

Figure 1: *The normalized radius (solid line, left scale) and internal pressure (dotted line, right scale) predicted numerically in one cycle of pressure for an argon bubble at P_A=0.93 atm, R_o=26 μm, =21 kHz. The bubble expands slowly when the bubble pressure is higher than the ambient pressure and collapse violently followed by three rebounds. The maximum pressure occurs during the first collapse of the bubble and peak pressures decreases significantly following each rebound. (a) results from the current model, (b) Kamath it et al.'s results (1993).*

3.2 Predicted Sonochemical Yields

The productions of radicals, *OH*, *H*, HO_2 and H_2O_2, in one cycle of driving pressure are plotted in Figure 2. In this study, the driving pressure has an amplitude of 0.93 *atm* at 21 *kHz* and the gas content is 50% H_2O vapor, 30% H_2 and 20% O_2. As shown, *H* and *OH* radicals inside the bubble increase rapidly during bubble collapse due to the dissociation of H_2O vapor. During the expansion and early stage of collapse, *OH* radicals recombine and form H_2O_2 and *H* radicals react with oxygen forming HO_2 as indicated in Equations (9) and (10). Consequently, the *H*, and *OH* radicals both decrease and HO_2 and H_2O_2 both increase accordingly. The *H* radical concentration increases gradually following each rapid decrease because of the reaction mecha

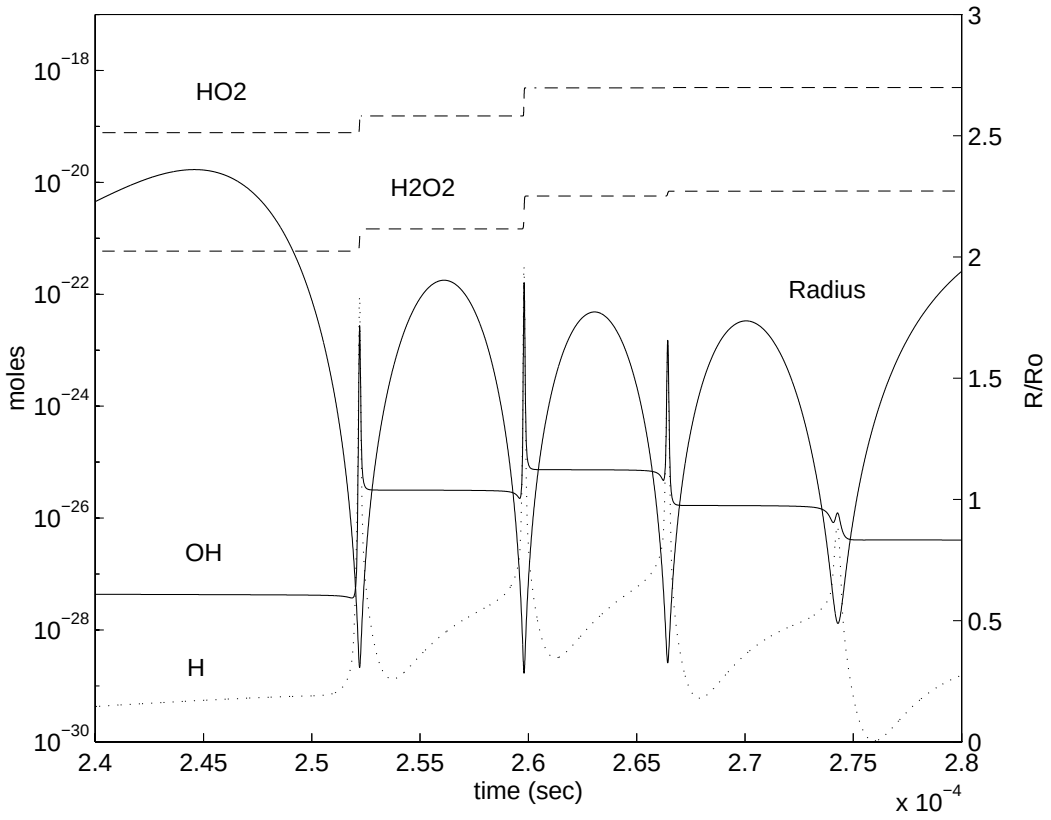

Figure 2: *The productions of radicals, OH, H, HO_2, and H_2O_2, during a typical cycle of bubble oscillation at P_A=0.93 atm, R_o=26 μm, f=21 kHz and a gas content of 50% water vapor, 30% H_2 and 20% O_2. H and OH radicals inside the bubble increase rapidly during bubble collapse due to the dissociation of H_2O. During the expansion and early stage of collapse, OH radicals recombine and form H_2O_2 and H radicals react with oxygen forming HO_2. As a result, the H and OH radicals both decrease and HO_2 and H_2O_2 both increase accordingly.*

An unusual phenomenon illustrated in this plot, is the accumulation of *OH* over multiple bubble oscillations. This accumulation is shown in detail in Figure 3 where the accumulation of the *OH* inside a 26 μm bubble oscillating over several cycles at a driving pressure of 0.93 *atm* and 27 *kHz* is illustrated. Each step increase in *OH* radicals corresponds to the most violent collapse of the bubble in one cycle of the driving pressure. This phenomenon is the result of the sudden drop in vapor density as the bubble expands.

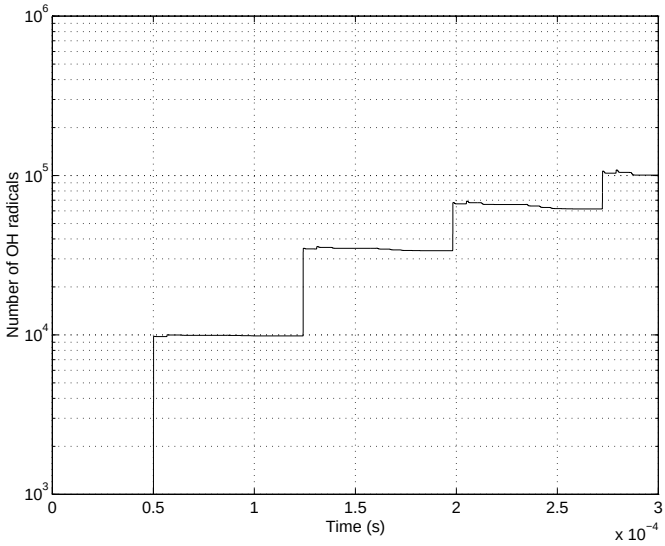

Figure 3: *Number of OH radicals produced in an argon bubble over several cycles of driving pressure at P_A=0.93 atm, R_o=26 μm, f=27 kHz. Each step increase in OH radicals corresponds to the most violent collapse of the bubble in one cycle of the driving pressure. The accumulation of OH radicals is due to a sudden drop in vapor density as the bubble expands.*

During bubble collapse, the vapor temperature and density is high resulting in a high rate of *OH* production. During expansion, the density of vapor drops as the temperature in the bubble decreases and the bubble radius increases. This drop in density slows *OH* recombination. Thus, there is a net increase in *OH* concentration inside the bubble with each bubble collapse. This effect is undoubtedly amplified in the result shown in Figure 3 since species transport to the bulk solution is not taken into account. It is likely that with transport a stable cavitation bubble in an acoustic field will accumulate *OH* asymptotically achieving a steady state concentration that is somewhat less than the level indicated.

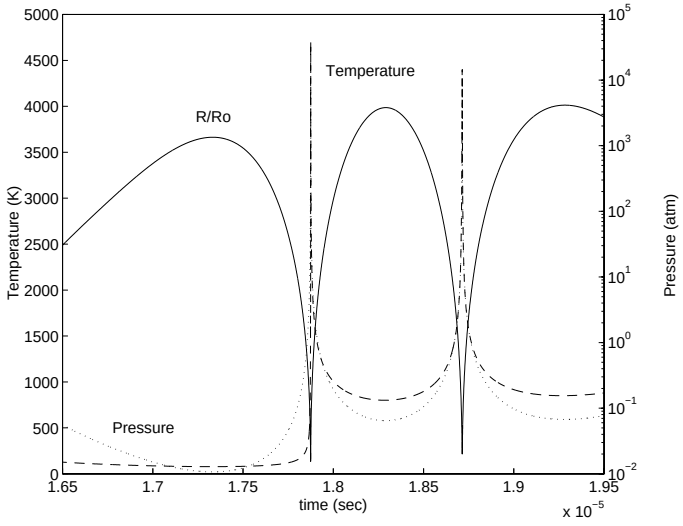

Figure 4: *Normalized bubble radius (solid line), temperature (dash line) and pressure (dotted line) variations as water is sonicated under a mixture of 60% H_2 and 40% O_2 at P_A=1.09 atm, Ro=2 μm, f=300 kHz. The bubble temperature remains relatively high (around 1000 °K) between the two collapses even when the bubble radius is three times larger than its initial value.*

Perhaps a more unusual phenomenon, which the current model predicts as a result of the coupling of chemical kinetics and bubble dynamics, can be seen in Figure 4. Here, two consecutive bubble collapses and the predicted bulk vapor temperature and pressure are plotted for a 2 μm bubble driven by a 1.1 *atm*, 300 *kHz* acoustic field. The bubble temperature remains relatively high (around 1000 °K) between the two collapses even when the bubble radius is three times larger than its initial value. This unusual phenomenon occurs, not because of a change in the bulk specific heat of the vapor in the bubble, but as a consequence of a net decrease in the number of moles in the vapor phase (see Figure 5). As illustrated in Figure 6, during the first bubble collapse, there is a sharp rise in the concentration of HO_2, OH, and H_2O_2 and a corresponding drop in O_2 and H_2. The net change is an overall drop in total moles of vapor. As indicated in Figure 5, the net specific heat of the vapor remains, on average, constant. Thus, there is a rise in the average bulk temperature of the vapor in the bubble. The effect of a rise in average temperature and drop in total species concentration offset one another and result in little change in peak pressure and temperature occurring in the second consecutive bubble collapse. Because of the drop in O_2 and H_2 concentrations during the first bubble collapse, there is little change in vapor composition from subsequent collapses although the temperature reached during these collapses can be on the same order as that occurring during the first collapse.

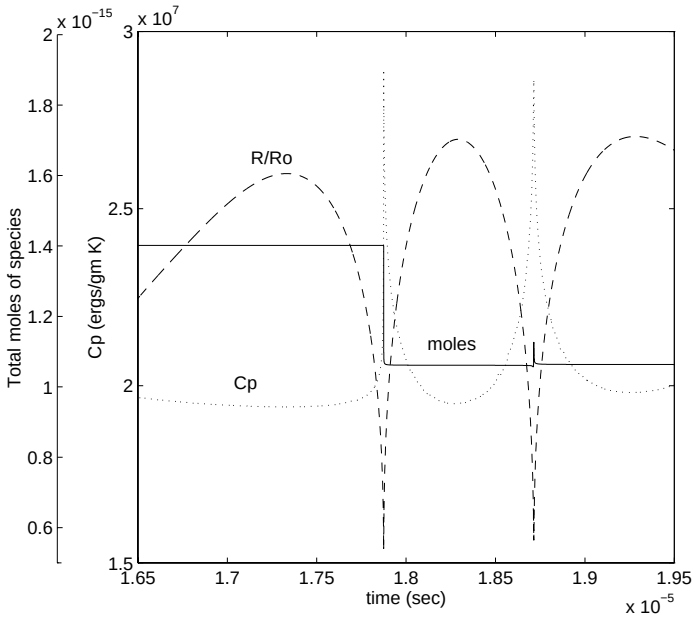

Figure 5: *Total moles of radicals and molecules (solid line) and the bubble heat capacity at constant pressure (dotted line) under the same conditions as in Figure 4. Normalized bubble radius is plotted (dashed line) as a reference. Heat capacity varies as the mass fraction of radicals and molecules changes during bubble collapse. There is an overall drop in total moles of radicals and molecules following the first collapse.*

3.3 Comparison with Experimentally Measured Sonochemical Yields

Few experimental measurements are available that show extensive sonochemical data for comparison. Henglein and his colleague conducted a number of experiments to study the production rate of H_2O_2 when water is sonicated under different gas compositions[9,10]. While

the present model focuses on a single bubble, Henglein's data were obtained from a bulk solution. Therefore, an exact comparison between this model and experimental results is impossible. It is believed, however, that the trends of the sonochemical yields in a single bubble are consistent with that in bulk production.

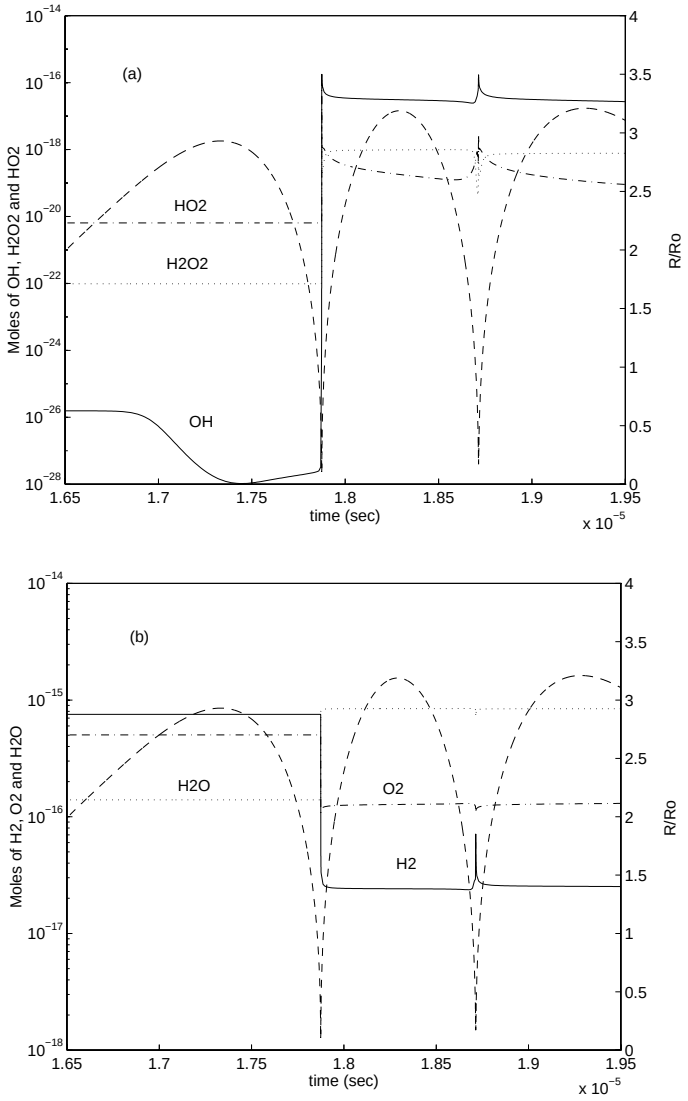

Figure 6: *The production of radicals and molecules inside the bubble as a function of time under the same conditions as in Figure 4. Normalized bubble radius is plotted (dashed line) as a reference. During the first bubble collapse, there is a sharp rise in the concentration of HO_2 (dash-dot line in (a)), OH (solid line in (a)) and H_2O_2 (dotted line in (a)) and a corresponding drop in O_2 (dash-dot line in (b)) and H_2 (solid line in (b)). Note that the water vapor concentration increases after the first bubble collapse.*

Figures 7(a) and 8(a) show the production rate of H_2O_2 as a function of H_2/Ar (O_2/Ar) and H_2/O_2 gas mixtures respectively measured by Henglein. These experimental data show that, for the H_2/Ar gas mixture, the production rate of H_2O_2 decreases rapidly as H_2 concentration increases. For the O_2/Ar gas mixtures, the production rate of H_2O_2 first increases as O_2 concentration increases until the volume percentage of the oxygen reaches 30 percent. It then

decreases as O_2 concentration increases further. When the gas atmosphere is changed to a hydrogen-oxygen, H_2/O_2, mixture, the production rate of H_2O_2 exhibits an unusual double peak feature. Henglein suggested that the high thermal conductivity of hydrogen, which lowers the temperature in the compressed cavitation bubbles at higher hydrogen concentrations, is responsible for the decrease in H_2O_2 for hydrogen concentrations above 30 percent. The current model indicates that thermal conductivity of hydrogen may not be the factor that causes this decrease in H_2O_2. The model indicates instead that species interactions under these conditions are the primary factor for this behavior.

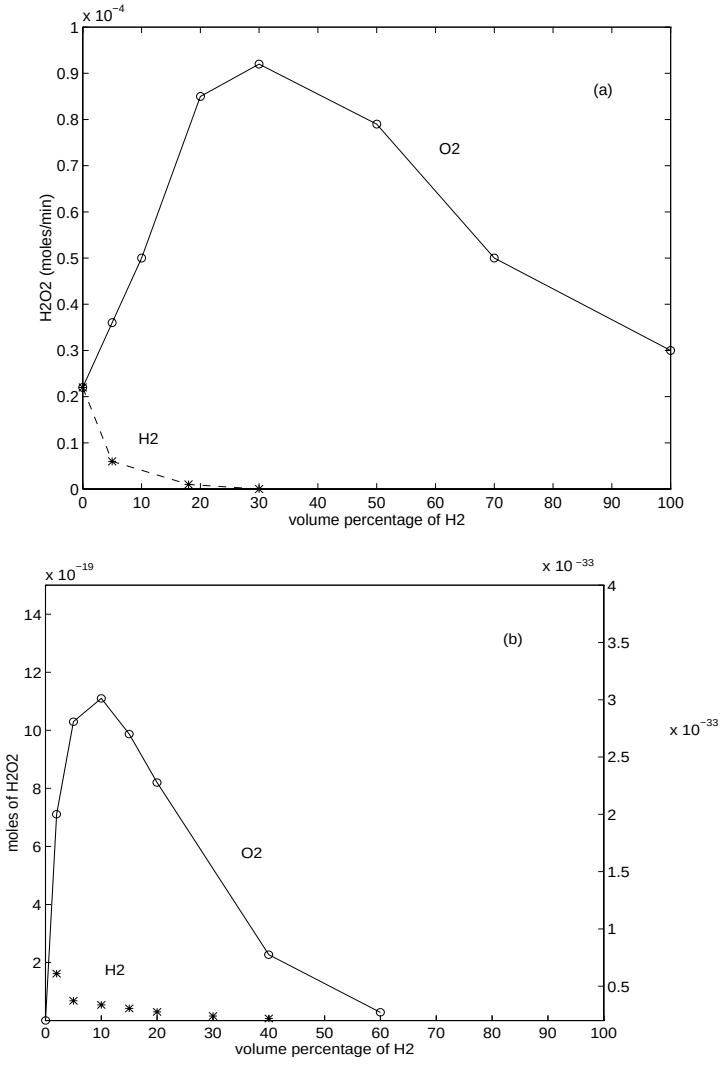

Figure 7: *Comparison of the production of hydrogen peroxide in water sonicated under a mixture of H_2/Ar and O_2/Ar at P_A=1.09 atm, f=300 kHz between (a) experimental results from Henglein (1993) and (b) numerical predictions. Though an exact comparison is not possible, the plot indicates that the trends of the sonochemical yields in a single bubble (numerical predictions) and those in bulk production (measurements) are very similar. As illustrated, the production rate of H_2O_2 decreases rapidly as H_2 concentration increases; the production rate of H_2O_2 first increases as O_2 concentration increases and then decreases with a further increase in O_2 concentration.*

Figure 7(b) shows the predicted formation of H_2O_2 in water sonicated under a gas mixture of H_2/Ar (O_2/Ar). The acoustic frequency of the sound field in this study is 300 *kHz*, which is the same as that used in Henglein's experiments. Other parameters are specified as: R_o is 2 μm, the viscosity of the surrounding liquid is 0.001 *Kg/(s·m)*, and the amplitude of the sound is 1.09 *atm*. Compared to Henglein's results, shown in Figure 7(a), the predicted results show similar characteristic features. The mechanism which results in the rapid decrease in H_2O_2 for the H_2/Ar gas mixture can be described by the following,

$$OH^{\bullet} + H_2 \rightarrow H_2O + H^{\bullet}$$

OH radicals react with H_2 as H_2 concentration increases, which makes the H_2O_2 formation mechanism from the combination of *OH* radicals shown in Equation (9) less effective. While for the O_2/Ar gas mixture, the related mechanism is

$$O_2 + H^{\bullet} \rightarrow HO_2^{\bullet}$$

As *H* radicals react with oxygen, more HO_2 is produced when the oxygen concentration is relatively low. Consequently, more H_2O_2 is produced according to the mechanism shown in Equation (12). When the O_2 concentration is high, the mechanism of dissociation of H_2O is less effective due to the low ratio of specific heat of oxygen compared to that of argon.

When the gas composition is H_2/O_2, the predicted yield of H_2O_2 at the rebound (marked as 1) and early stage of collapse (marked as 2) is shown in Figure 8(b). Markers 1 and 2 correspond to stages where bubble temperature is around 1000 °K. The double peak feature of H_2O_2 formation is captured in the numerical modeling. The mechanisms, which relate to the initial increase in H_2O_2 formation and the decrease in H_2O_2 formation when H_2 concentration is over 50 percent, are described by Hart and Henglein[7]. They propose that the decrease in thermal conductivity of hydrogen at lower concentrations is responsible for this unusual behavior. Even when the thermal conduction of the vapor in the bubble is removed from the energy equation, however, the current model shows qualitatively the same trend as the experimental results. Thus, it appears unlikely that Hart and Henglein's explanation for this behavior is entirely correct. While, indeed, the thermal conductivity does play a role in this behavior, the model indicates that it is the heat release due to the formation of water from hydrogen and oxygen that is the primary contributing factor. At higher temperatures, H_2O_2 is unstable and disassociates resulting in a net drop in concentration. As the concentration of H_2 relative to O_2 is increased or decreased from a 35% H_2, 65% O_2 ratio, the reaction of H_2 and O_2 to H_2O is limited in accordance with concentration ratios and the resulting concentration of H_2O_2 increases and the peak temperatures reached during bubble collapse decreases.

As shown in Figure 8(b), the formation of H_2O_2 is higher at the early stage of collapse than at the rebound stage when bubble temperatures at these two stages are the same. During bubble rebound, radicals recombine to form H_2O and reaction rate slows as bubble volume increases and species concentration decreases. During the collapse stage, concentration of radicals becomes very high which results in a higher formation of H_2O_2 than during expansion.

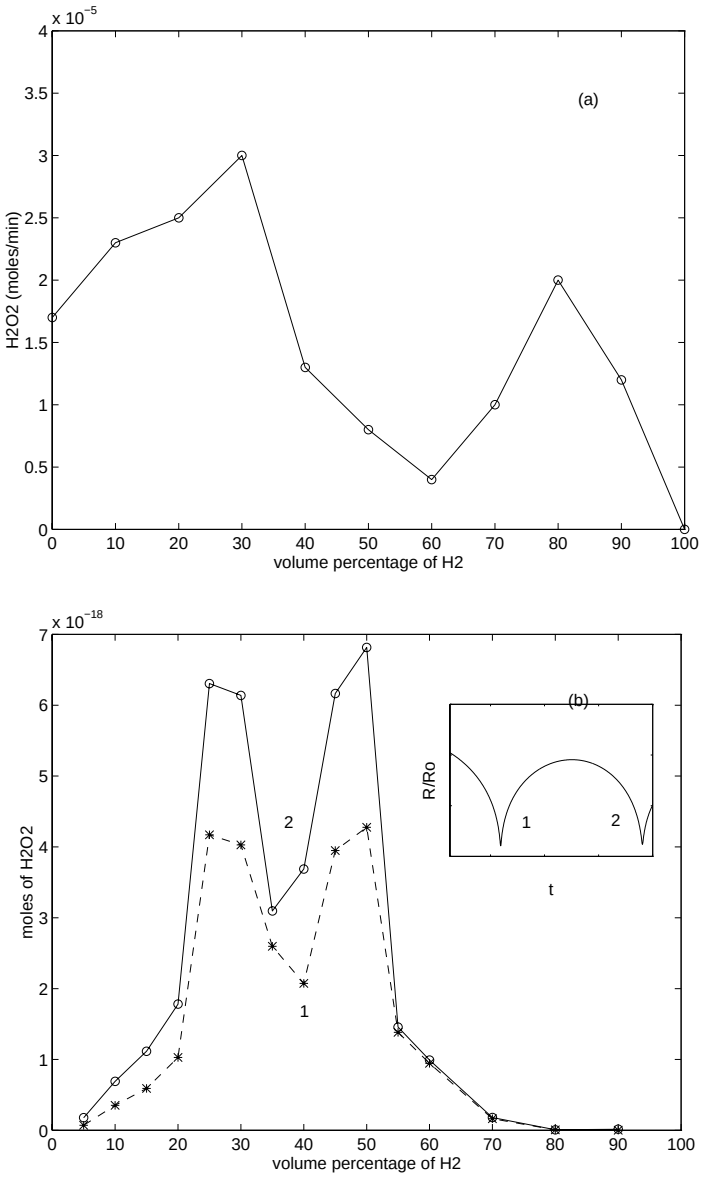

Figure 8: *Comparison of the production of hydrogen peroxide in water sonicated under mixture of H_2/O_2 at P_A=1.09 atm, f=300 kHz between (a) experimental results from Henglein (1993) and (b) numerical predictions. Double peak formation of H_2O_2 is observed in both numerical prediction and experimental measurement.*

While the present model does not account for mass transfer, it appears that species transport to the bulk solution may occur primarily during the final stages of bubble collapse when the observed characteristic species concentrations occur in the vapor phase. A thermal boundary layer near the wall of the bubble prevents the liquid surrounding the bubble from reaching temperatures necessary to generate the experimentally measured concentrations of H_2O_2. During the final stage of bubble collapse, species concentration, vapor temperature, and the bubble surface area to volume ratio is high. Thus, a diffusional transport mechanism may be responsible for the exchange of species from the vapor to the liquid phase at this location of the bubble oscillation cycle.

4 SUMMARY AND CONCLUSIONS

Presented is a model that directly couples the dynamics and the chemical kinetics of a single cavitation bubble in a sound field. This model is verified with available experimental data. Comparisons with previous theoretical work by Kamath *et al.* and experimental work by Henglein *et al.* show that this model not only captures the main characteristics of the dynamics of bubble collapse but also qualitatively predicts detailed behavior of sonochemical yields produced under varying dissolved gas content and composition.

The present model provides a tool to study the parametric effects on sonochemical processes. Investigated are the effects of gas compositions on sonochemical yields associated with bubble dynamics and the effect of the chemical reactions on the bubble dynamics. The accumulation of *OH* radicals inside cavitation bubbles and the nonlinearly of bubble motion are captured. Suggested is a new mechanism, heat release due to formation of water from hydrogen and oxygen that results in an unusual fall and then rise in the formation of hydrogen peroxide as an increasing amount of hydrogen/oxygen mixture is dissolved into solution. The model shows that, despite its volatility, *OH* can accumulate in the vapor phase of the bubble increasing in concentration with each oscillation. This unusual phenomenon is due to the rapid expansion of the bubble after collapse dropping species concentration and thus slowing reaction rates during the rarefaction phase of the bubble oscillation cycle.

As the model presented accounts only for the chemistry occurring in the vapor phase of a single cavitation bubble and does not account for the transport of species into solution, it fails to provide a tool for investigating overall sonochemical reaction rates. Despite this, it provides a means of observing fundamental parametric relationships and investigating chemical kinetics during bubble collapse.

REFERENCES

[1] T.J. Mason and J.P. Lorimer, Sonochemistry: Theory, Applications And Uses Of Ultrasound In Chemistry, (Ellis Horwood Limited 1988).

[2] M.S. Plesset, Journal of Applied Mechanics **16**, 277-282 (1949).

[3] L. Rayleigh, Phil. Mag. **34**, 94-98 (1917).

[4] D.F. Gaitan, L.A. Crum, C.C. Church and R.A. Roy, Journal of the Acoustical Society of America **91**, No.6, 3166-3183 (1992).

[5] Y. Matsumoto and F. Takemura, JSME International Journal, Series B, Fluids and Thermal Engineering **37**, No.2, 288-296 (1994).

[6] M. Anbar and I. Pecht, Journal of Physical Chemistry **68**, No.2, 352-355 (1964).

[7] E.H. Hart and A. Henglein, Journal of Physical Chemistry **91**, 3654-3656 (1987).

[8] A. Henglein, Advances in Sonochemistry **3**, 17-83 (1993).

[9] K.S. Suslick, Mingming Fang and T. Hyeon, Journal of the American Chemical Society **118**, 119-160 (1996).

[10] K.S. Suslick, S.B. Choe, A.A. Cichowlas and M.W. Grinstaff, Nature **353**, 414-416 (1991).

[11] K.S. Suslick, S.J. Doktycz and E.B. Flint, Ultrasonics **28**, 280-290 (1990).

[12] E.B. Flint and K.S. Suslick, Science **253**, No.5026, 248-249 (1991).

[13] V.A. Kamath, A. Prosperetti and F.N. Egolfopoulos, Journal of the Acoustical Society of America **94**, No. 1, 248-260 (1993).

[14] R.J. Kee, F.M. Rupley and J.A. Miller, CHEMKIN, a FORTRAN chemical kinetics package for the analysis of gas-phase chemical kinetics, (Sandia National Laboratories, 1994).

[15] G.I. Kuvshinov, Journal of Engineering Physics **60**, No.1, 34-37 (1991).

[16] S. Fujikawa and T. Akamatsu, Journal or Fluid Mechanics **97**, 481-512 (1980).